

Article

Design of a Compact Quad-Channel Microstrip Diplexer for L and S Band Applications

Sobhan Roshani ¹, Salah I. Yahya ^{2,3}, Yaqeen Sabah Mezaal ⁴, Muhammad Akmal Chaudhary ⁵,
Aqeel A. Al-Hilali ⁶, Afshin Mojirleilani ¹ and Saeed Roshani ^{1,*}

¹ Department of Electrical Engineering, Kermanshah Branch, Islamic Azad University, Kermanshah 6718997551, Iran

² Department of Communication and Computer Engineering, Cihan University-Erbil, Erbil 44001, Iraq

³ Department of Software Engineering, Faculty of Engineering, Koya University, Koya KOY45, Iraq

⁴ Medical Instrumentation Engineering Department, Al-Esraa University College, Baghdad 10011, Iraq

⁵ Department of Electrical and Computer Engineering, College of Engineering and Information Technology, Ajman University, Ajman 346, United Arab Emirates

⁶ College of Medical Techniques, Al-Farahidi University, Baghdad 10011, Iraq

* Correspondence: s_roshany@yahoo.com

Abstract: In this paper, two novel dual-band bandpass filters (BPFs) and a compact quad-channel diplexer working at 1.7/3.3 GHz and 1.9/3.6 GHz are proposed. In the proposed diplexer design, triangular loop resonators and rectangular loop resonators are used together to reduce the circuit size and improve diplexer performances. Insertion loss (IL) and return loss (RL) of the proposed diplexer are better than 0.8 dB and 21 dB, respectively, at these four operating frequencies. Output ports isolation parameter is better than 30 dB. With the achieved specifications, the proposed diplexer can be used in L and S band applications.

Keywords: bandpass filter; diplexer; quad-channel; resonator; coupled lines; microstrip; insertion loss; return loss



Citation: Roshani, S.; Yahya, S.I.; Mezaal, Y.S.; Chaudhary, M.A.; Al-Hilali, A.A.; Mojirleilani, A.; Roshani, S. Design of a Compact Quad-Channel Microstrip Diplexer for L and S Band Applications. *Micromachines* **2023**, *14*, 553. <https://doi.org/10.3390/mi14030553>

Academic Editors: Hongping Hu, Pei-Hsun Wang, Zhenghua Qian and Aiqun Liu

Received: 3 January 2023

Revised: 4 February 2023

Accepted: 24 February 2023

Published: 26 February 2023



Copyright: © 2023 by the authors. Licensee MDPI, Basel, Switzerland. This article is an open access article distributed under the terms and conditions of the Creative Commons Attribution (CC BY) license (<https://creativecommons.org/licenses/by/4.0/>).

1. Introduction

Diplexers are three-port devices, which are widely used in microwave circuits and systems. The diplexer devices split input signal from the common input port into two separate channels with two different desirable operating frequencies [1,2]. Microstrip diplexers are considered as key component in many communication systems. In many applications, diplexers allow a single antenna to receive and transmit on different frequencies. Moreover, diplexers will provide the ability for an antenna to receive and transmit simultaneously [3]. In recent reported works, hairpin resonators [4], stepped-impedance resonators [5], bandpass filters (BPFs) [6], square ring resonators [7] approaches are used to design and improve the performance of the diplexers. In [4], two hairpin line resonators are used in the diplexer structure to obtain two wide operating bands. Five stepped-impedance resonators are used to achieve a diplexer with compact size and high isolation in [5].

Recently, optimization algorithms [8,9] and neural network techniques have been used to improve performance of electronic circuits, such as in [10–14], which also have been used in the designing of the BPF [15] and coupler [16]. In [15], a narrow band BPF at 2.2 GHz is designed, with a hairpin structure. An artificial neural network (ANN) is used to optimized BPF, and in [16], an ANN model is used to find transfer function of the branch line coupler. Additionally, higher frequencies for filters and resonators have been achieved using optical fiber substrates [17–22].

Additionally, lumped reactive components such as capacitors and inductors are used in microwave circuits to provide a bandpass response, such as in [23–25]. Applied lumped reactive components increase insertion loss, which is not desirable.

Different kinds of resonators are also used for the performance improvement of the frequency response [26–36]. Different shapes of the resonators have been recently presented, such as U-shaped [26], T-shaped [27], Pi-shaped, [28] stepped-impedance [29], and patch resonators [30,31]. In [30], patch resonators are used to have a filtering response.

This paper presents a compact diplexer formed by two dual-band bandpass filters using triangular loop resonators and rectangular loop resonators operating at 1.7/3.3 GHz and 1.9/3.6 GHz. The proposed quad-channel diplexer is designed for L band and S band applications, which includes 1–2 GHz for L band and 2–4 GHz for S band.

2. Bandpass Filters Design

The proposed diplexer consists of two dual-band BPFs. At the first step of design process, the BPFs structure are introduced. The BPFs are designed using triangular loop and rectangular loop resonators to form a microstrip quad-channel diplexer for L band and S band applications. At the first step, coupled lines and rectangular loop resonators are combined to provide a dual-band resonator, named resonator1. The structure and response of resonator1 are depicted in Figure 1a,b. As seen, resonator1 provides two narrow operating bands at 2.4 GHz and 3.8 GHz. Additionally, the resonator1 creates a transmission zero (TZ) at 6.6 GHz, which provides a stop band near this transmission zero.

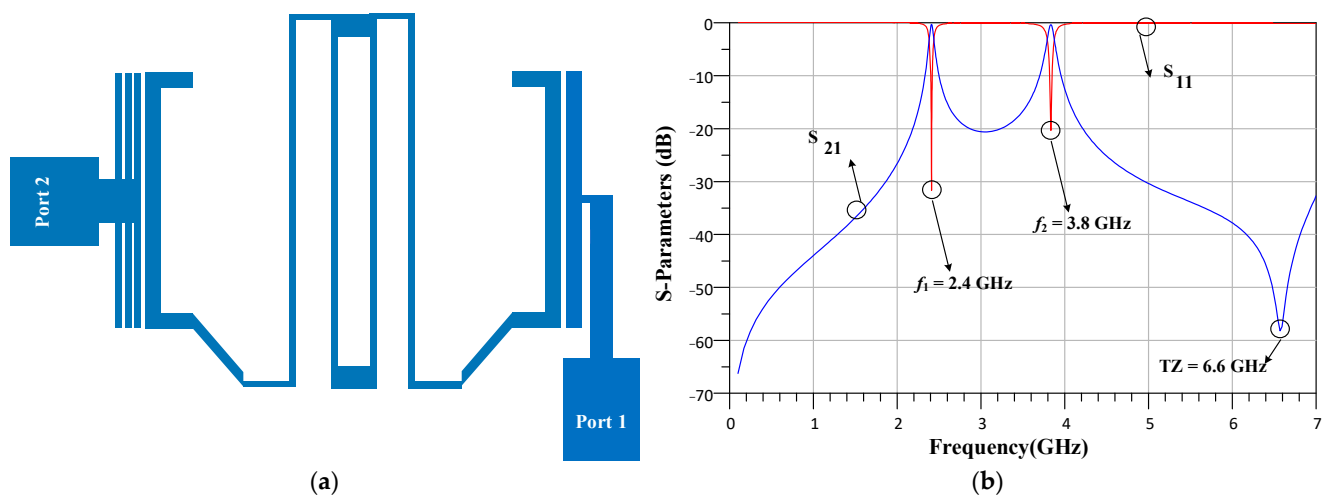


Figure 1. The (a) structure and (b) response of resonator1.

At the second step, triangular loop resonators and Pi-shaped resonators are incorporated to form resonator2. The structure and response of resonator2 are depicted in Figure 2a,b. Resonator2 provides two operating bands at 1.9 GHz and 5.2 GHz. As seen, resonator2 cannot provide a stopband with high attenuation level.

In order to create a compact BPF with high attenuated stop band, resonator1 and resonator2 are combined to form the final structure of the first BPF. Figure 3 shows the structure of the first designed band-pass filter, which passes signals at 1.9 GHz and 3.6 GHz frequencies and suppresses other frequencies. The simulated frequency responses of this proposed filter are depicted in Figure 4. The insertion losses (IL) at the operating frequencies are 0.52 dB and 0.76 dB, and the return losses (RL) parameter values are better than 40 dB and 33 dB, respectively.

In the structure of the proposed BPF shown in Figure 3, there are two space gaps, which creates coupling. These gaps, which are demonstrated with “S”, are very important. As seen in Figure 5, by tuning the values of S, the operating frequency and the IL can be adjusted. The lowest insertion loss is obtained for $S = 0.1$ mm.

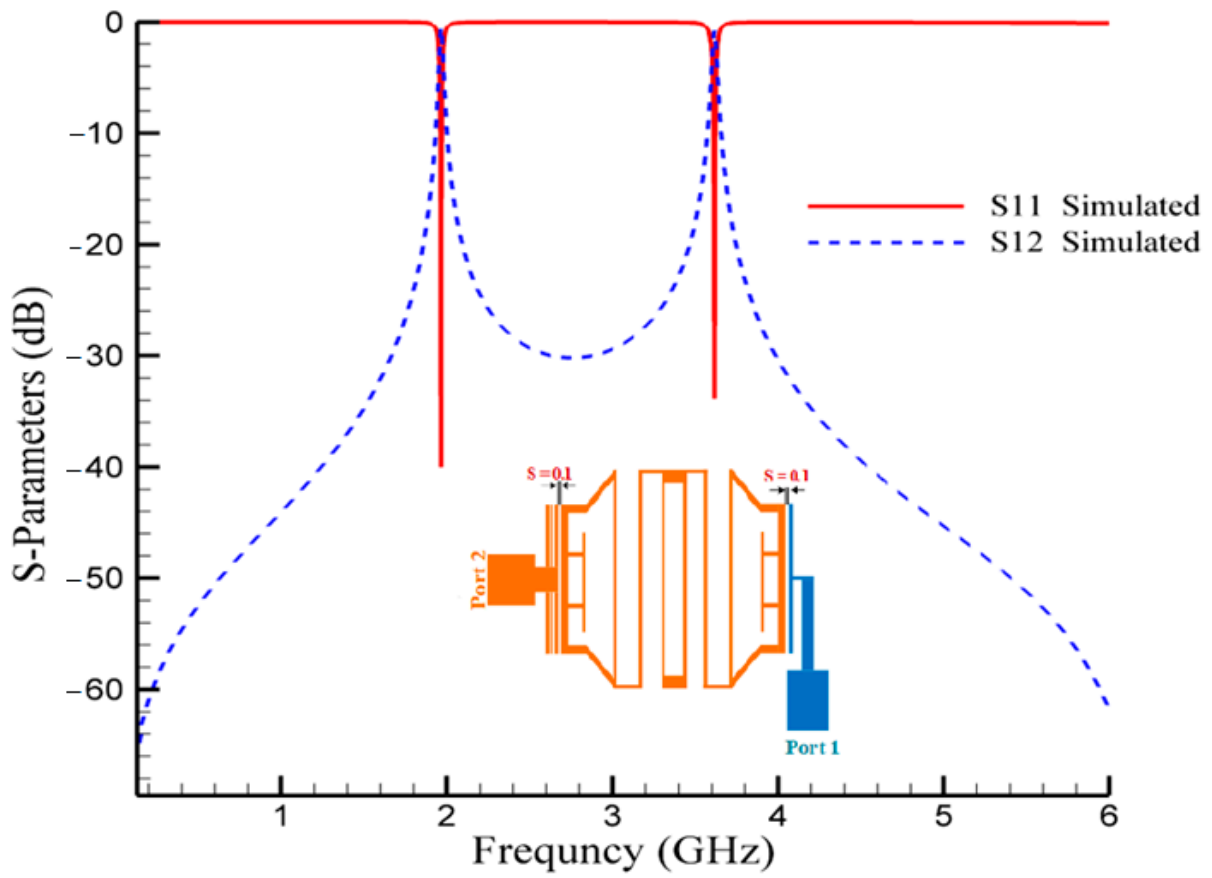


Figure 4. Simulated frequency responses of the first proposed BPF at 1.9/3.6 GHz.

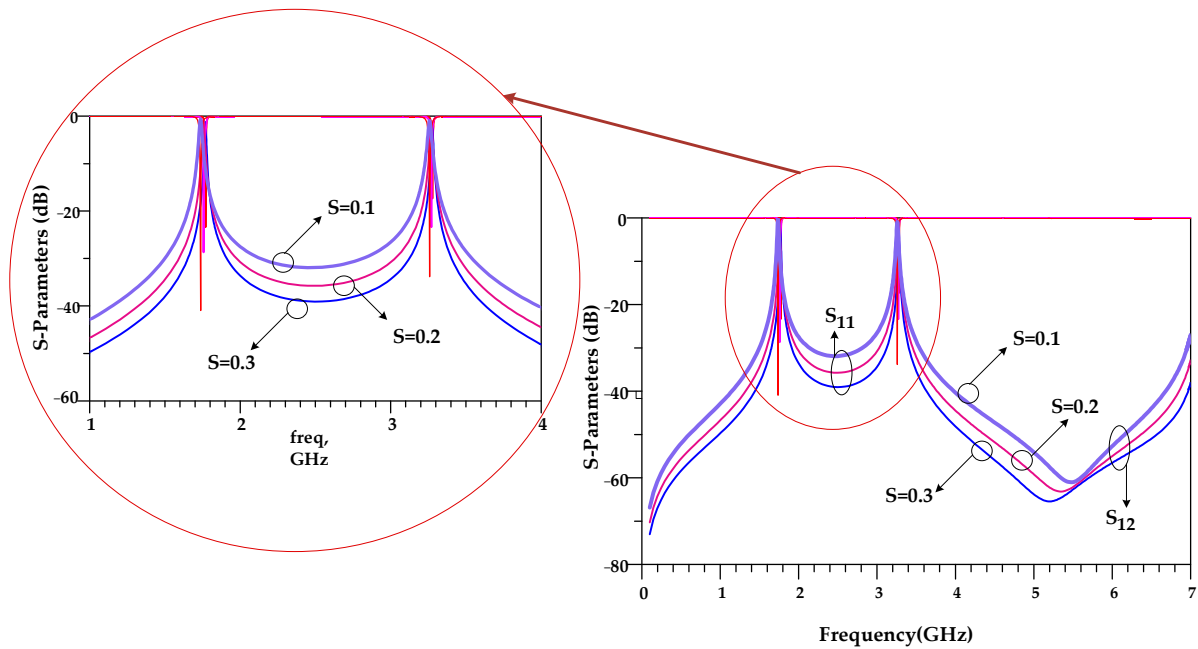


Figure 5. Effects of gap space (S) in the first proposed BPF at 1.9/3.6 GHz.

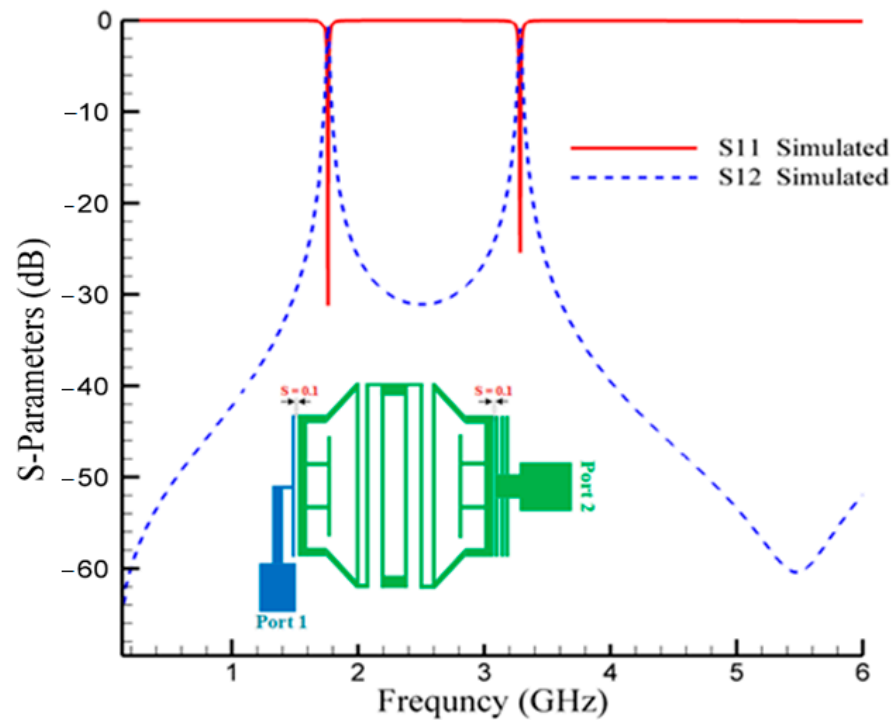


Figure 8. Simulated frequency responses of the second proposed BPF at 1.7/3.3 GHz.

Like the first BPF, in the structure of the proposed second BPF, as seen in Figure 7, there are two space gaps, which creates coupling. These gaps, which are demonstrated with “S”, are very important. As seen in Figure 9, by tuning the values of S, the operating frequency and the IL can be adjusted. The lowest insertion loss is obtained for S = 0.1 mm.

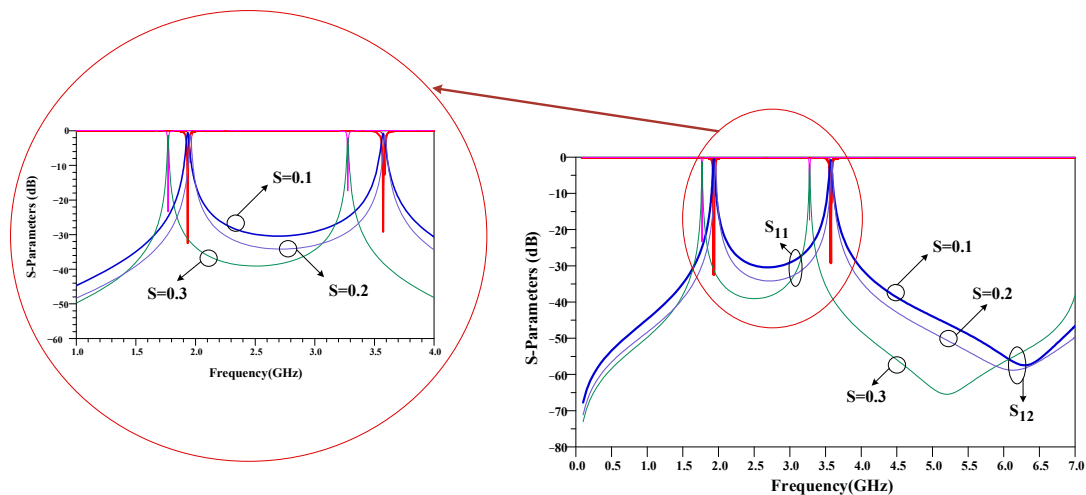


Figure 9. Effects of gap space (S) in the second proposed BPF at 1.7/3.3 GHz.

The design procedure of the proposed diplexer is depicted in Figure 10. In step1, rectangular loop and triangular loop resonators are designed. In step2, the designed rectangular loop and triangular loop resonators are combined to form the main dual-band proposed BPF. Then, based on the proposed main dual-band BPF, two BPFs are presented to provide four channels for the diplexer, as shown in step3. Additionally, in step4, the proposed quad-channel diplexer is presented by combining the two designed BPFs.

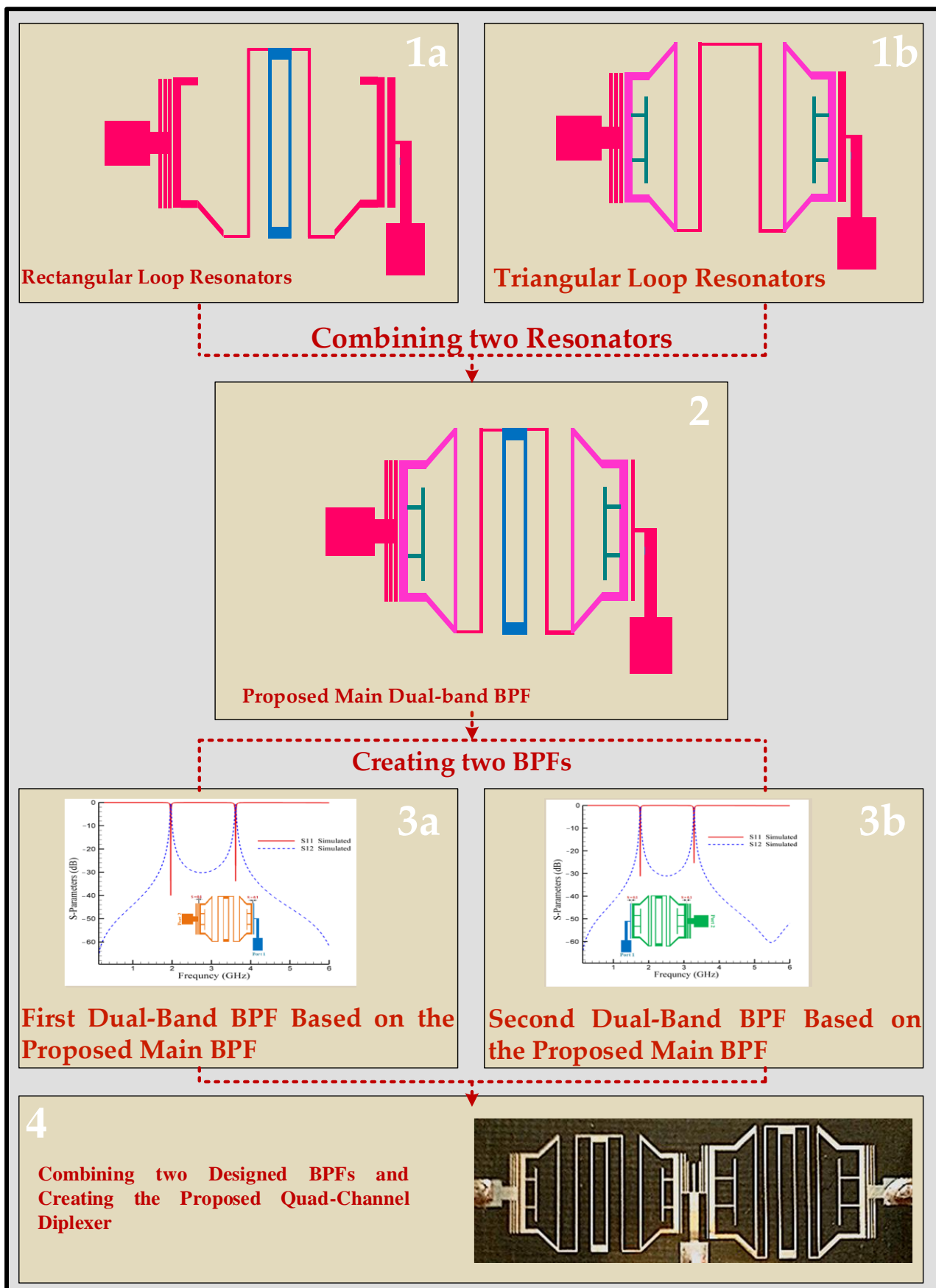


Figure 10. Design procedure of the proposed diplexer. The design steps of the proposed quad-channel diplexer are explained in four steps, which are indicated in the figure.

4. Results and Discussion

The final dimensions of diplexer are only $11.2 \text{ mm} \times 32.2 \text{ mm}$ ($0.0903 \lambda_g \times 0.259 \lambda_g$). Figure 13 shows the photograph of the fabricated diplexer. The proposed quad-channel diplexer, which is working at 1.7/3.3 GHz and 1.9/3.6 GHz, is designed and fabricated on a single layer of RT Duroid 5880 substrate with a relative electric constant of $\epsilon_r = 2.2$, $\tan\delta = 0.0009$, and thickness of 0.7874 mm.

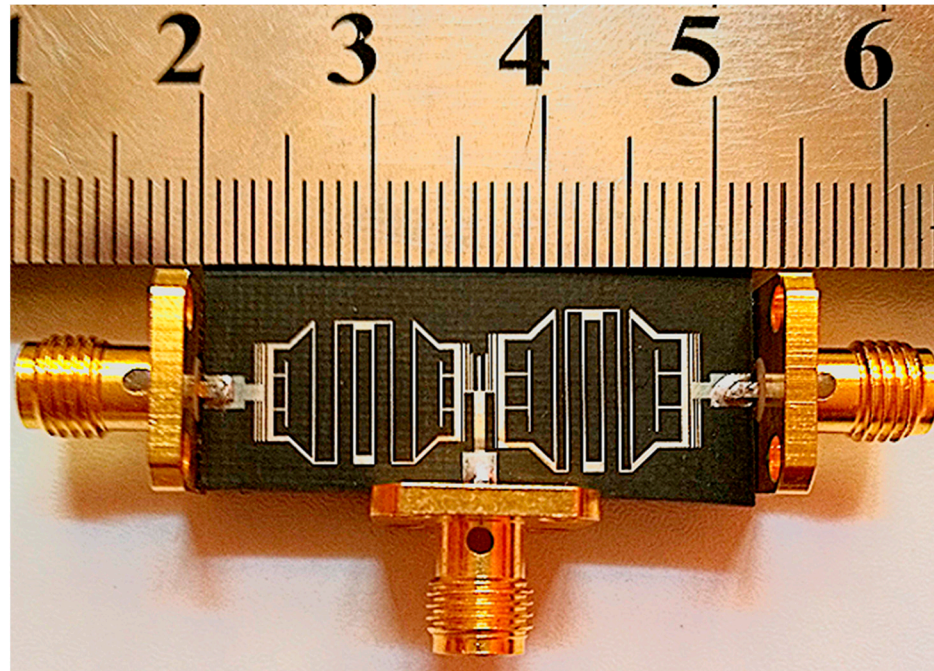


Figure 13. Fabricated photo of the proposed diplexer.

Port one represents the input port connected to the antenna, whereas port two and port three represent the output of the receiver filter and the input of the transmitter filter, respectively. All ports are designed for 50 Ohms impedance. Figure 14a,b shows the simulation and measurement results of the proposed diplexer. As seen in these figures, the proposed diplexer has two channels. The lower channel has two frequency bands 1.7/1.9 GHz, whereas the higher channel has two frequency bands 3.3/3.6 GHz. According to the fabrication measured results, the insertion loss parameters of the proposed diplexer are better than 0.6 dB at the lower channel and better than 0.8 dB at the higher channel. The measured return loss parameters are better than 20 dB and 25 dB at the lower and higher channel, respectively. Moreover, better than 30 dB ports isolation is obtained in the whole frequency band.

The simulated results of the proposed diplexer are listed in Table 1. As the results show, the proposed diplexer features very good specifications. In the lower bands (1.7 GHz and 1.9 GHz), the S_{21} parameter at 1.7 GHz is achieved (-0.55 dB), while the S_{31} parameter at 1.9 GHz is achieved (-0.55 dB); therefore, the insertion loss in lower bands is 0.55 dB. In the higher bands (3.3 GHz and 3.6 GHz), the S_{21} parameter at 3.3 GHz is achieved (-0.87 dB), while the S_{31} parameter at 3.6 GHz is achieved (-0.78 dB); therefore, the insertion loss in higher bands is better than 0.87 dB.

In the lower bands (1.7 GHz and 1.9 GHz), the S_{11} parameter for these two frequencies is achieved (-23.3 dB and -21.1 dB , respectively); therefore, the return loss in lower bands is better than 21 dB. In the higher bands (3.3 GHz and 3.6 GHz), the S_{11} parameter for these two frequencies is achieved (-25.64 dB and -25.67 dB , respectively); therefore, the return loss in higher bands is better than 25 dB.

Table 1. Specifications of the proposed diplexer.

Parameter	Unit	Lower Bands	Higher Bands
Frequency	GHz	1.7/1.9	3.3/3.6
Insertion loss	dB	0.55	Better than 0.87
Return loss	dB	Better than 21	Better than 25
Isolation	dB	Better than 30	Better than 31

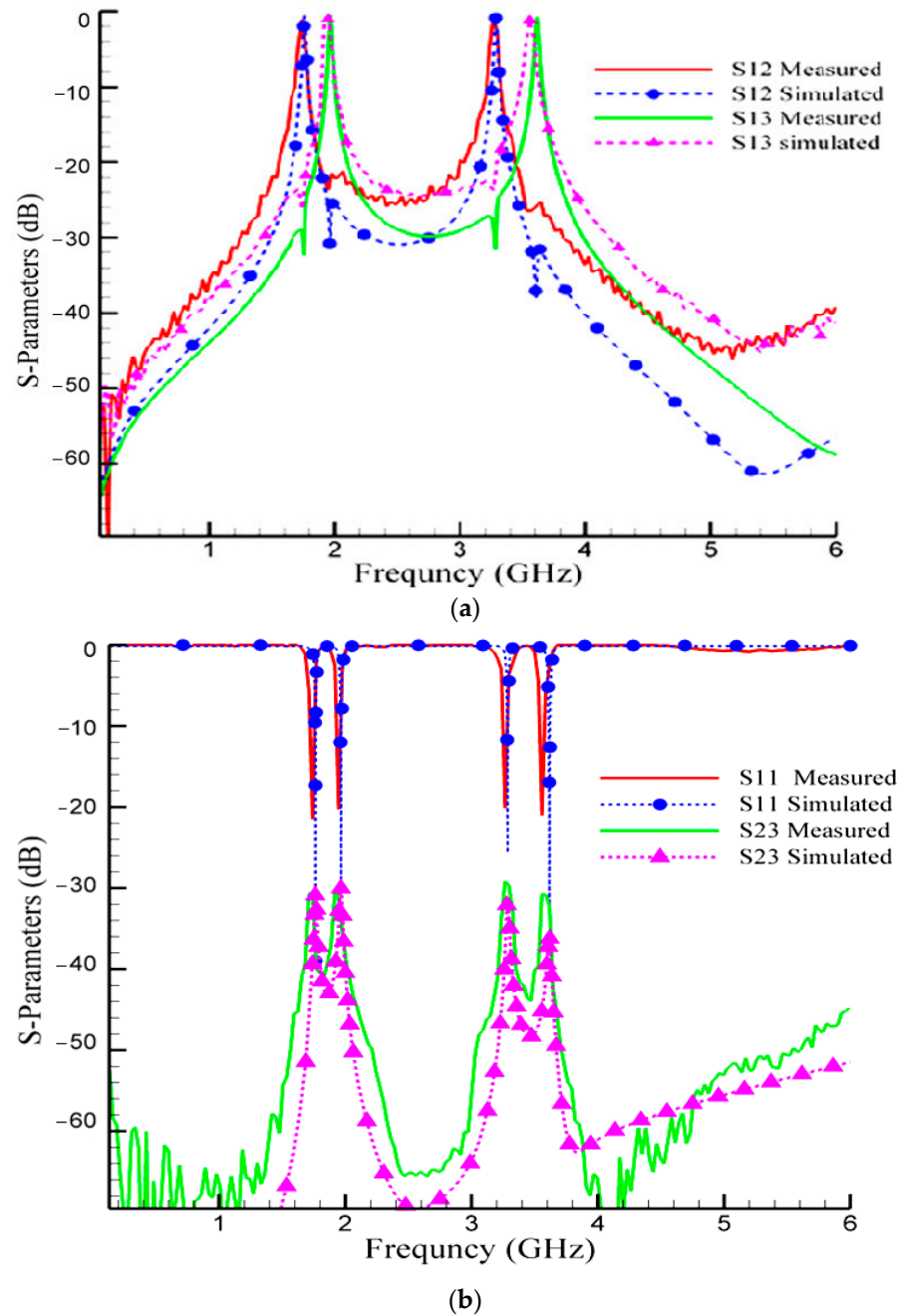
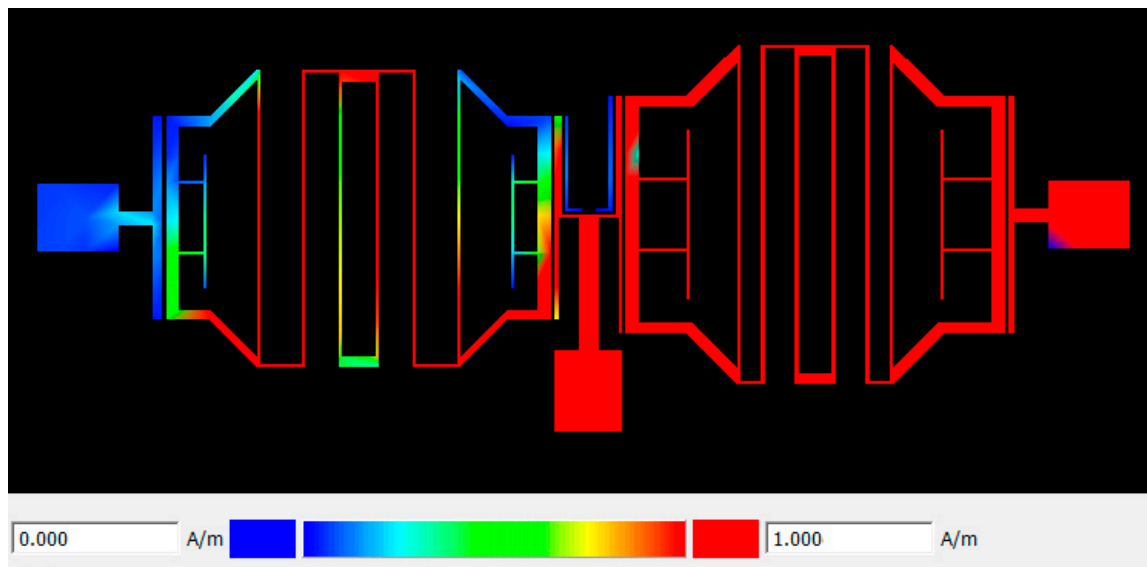


Figure 14. Simulation and measurement results of the proposed diplexer (a) scattering parameters (S_{12}, S_{13}) and (b) isolation parameter and input return loss (S_{11}, S_{23}).

In the lower bands (1.7 GHz and 1.9 GHz), the S_{23} parameter for these two frequencies is achieved (-30.83 dB and -30.04 dB, respectively); therefore, the isolation in lower bands

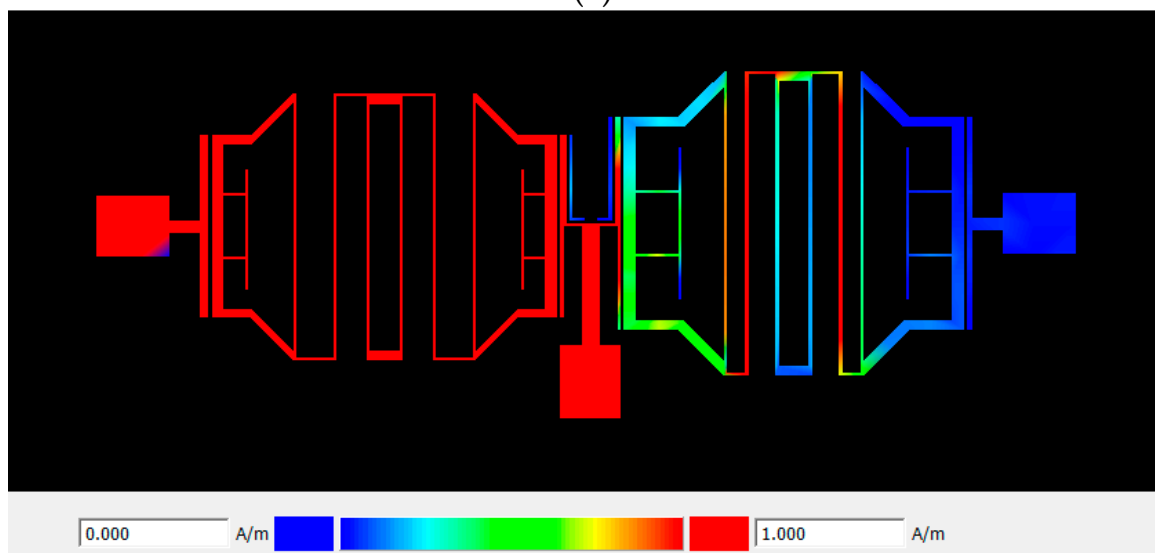
is better 30 dB. In the higher bands (3.3 GHz and 3.6 GHz), the S_{23} parameter for these two frequencies is achieved (-31.32 dB and -36.1 dB, respectively); therefore, the isolation in higher bands is better than 31 dB.

The surface current distributions in the proposed quad-band diplexer are demonstrated in Figure 15a–d. The proposed diplexer correctly works at four frequency bands of 1.7/1.9/3.3/3.6 GHz. As per the results shown in Figure 15a,c, the currents are correctly distributed uniformly at the port2 at the 1.7 GHz and 3.3 GHz frequencies and show that the currents have not reached the port3. Additionally, as seen in Figure 15b,d, the results show that the currents are correctly distributed uniformly at the port3 at the 1.9 GHz and 3.6 GHz frequencies and show that the currents have not reached the port2.



1.7 GHz

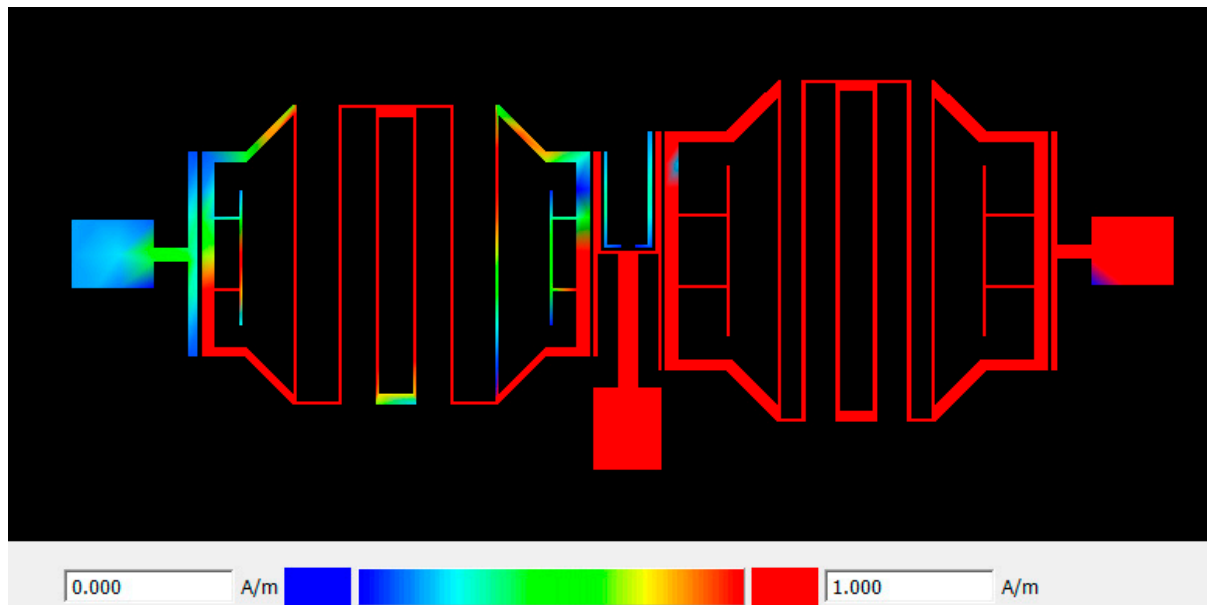
(a)



1.9 GHz

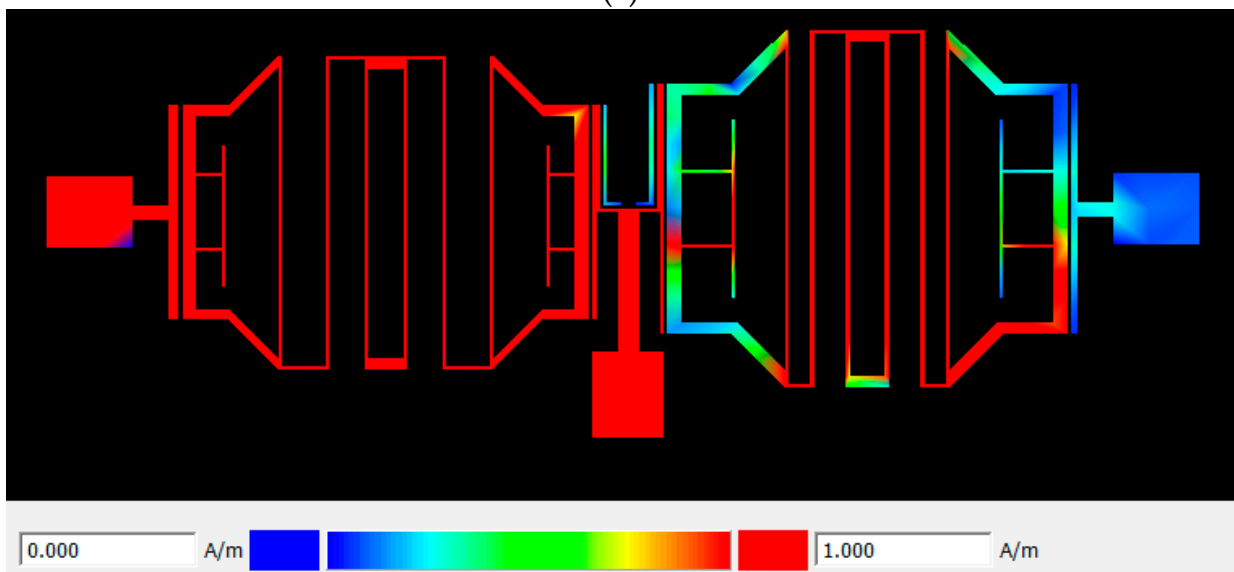
(b)

Figure 15. Cont.



3.3 GHz

(c)



3.6 GHz

(d)

Figure 15. Surface current distribution in the proposed diplexer at the frequencies of: (a) 1.7 GHz, first frequency band in port2; (b) 1.9 GHz, second frequency band in port3; (c) 3.3 GHz, third frequency band in port2; and (d) 3.6 GHz, fourth frequency band in port3. The maximum value of magnetic intensity is 1 A/M in all of cases.

The proposed diplexer has good features, where the S-parameters of the proposed device at the four operating frequencies are listed in Table 2.

A performance comparison between the designed diplexer with the previous reported diplexers is listed in Table 3. As seen in this table, most of the reported works focus on a dual-band diplexer, but the proposed diplexer operates at four frequencies. The proposed quad-channel diplexer shows good performance, compared to the reported works. The designed diplexer has the smallest size and lowest ILs, as compared with other reported works.

Table 2. Scattering parameters of the designed device.

S-Parameters (dB)	Frequency (GHz)			
	1.7	1.9	3.3	3.6
S_{11}	−23.30	−21.1	−25.64	−25.67
S_{12}	−0.55	−30.63	−0.87	−35.93
S_{13}	−29.44	−0.55	−30.20	−0.78
S_{23}	−30.83	−30.04	−31.32	−36.10

Table 3. Comparison between the designed devices with the previous duplexers.

Ref.	Lower Band (1) (dB)		Higher Band (1) (dB)		Lower Band (1) (dB)		Higher Band (1) (dB)		Lower Band (1) (dB)		Higher Band (1) (dB)		Lower Band (2) (GHz)		Higher Band (2) (GHz)		Size	
	IL_1	IL_2	IL_3	IL_4	IRL_1	IRL_2	IRL_3	IRL_4	I_1	I_2	I_3	I_4	f_1	f_2	f_3	f_4	mm ²	λ_g^2
This work	0.53	0.55	0.87	0.78	23	21	25	25	30	30	31	36	1.7	1.9	3.3	3.6	360.64	0.0233
[37]	0.8	1	0.7	1.5	24	21	23	22	50	30	45	30	1.5	2	2.4	3.5	1456	0.078
[38]	1.55	-	1.70	-	21	-	31	-	45	-	41	-	1.8	-	2.2	-	923.4	0.0667
[39]	2.2	-	2.1	-	27	-	26	-	30	-	30	-	1.82	-	2.41	-	859.32	0.0646
[40]	1.25	-	1.48	-	25	-	14	-	35	-	30	-	2.16	-	2.91	-	256	0.470
[41]	1.34	-	0.95	-	22	-	21	-	24	-	22	-	1.81	-	2.44	-	1040	0.179
[42]	2.1	-	2.1	-	20	-	20	-	20	-	20	-	1.75	-	1.85	-	918	0.0705
[43]	0.6	-	0.9	-	11	-	12	-	13	-	23	-	2.6	-	6	-	573.11	0.0809
[44]	1.5	-	1.3	-	21	-	21	-	31	-	35	-	2.34	-	2.59	-	816	0.1019

The parameter of IL_i represents insertion loss, IRL_i corresponds to input return loss, and I_i represents isolation.

5. Conclusions

In this paper, a compact quad-channel diplexer is designed, simulated and fabricated. The proposed structure is composed of two BPFs. In the proposed design, triangular loop and rectangular loop resonators are used together in order to reduce the circuit size and optimize the specifications of the proposed circuit. The proposed diplexer operates correctly at 1.7 GHz, 1.9 GHz, 3.3 GHz, and 3.6 GHz frequencies. The measured ILs are better than 0.8 dB, and the RLs are better than 20 dB at the four operating frequencies. Moreover, better than 30 dB ports isolation is obtained in the whole frequency band. With these specifications, the proposed diplexer can be useful for L band and S band applications.

Author Contributions: Conceptualization, S.R. (Saeed Roshani), A.M. and S.R. (Sobhan Roshani); Formal analysis, A.M. and M.A.C.; Methodology, S.I.Y. and Y.S.M.; Software A.A.A.-H., A.M., Y.S.M., A.A.A.-H. and S.R. (Sobhan Roshani); Validation, A.M. and Y.S.M.; Writing—original draft, S.R. (Saeed Roshani), A.M. and S.R. (Sobhan Roshani); Writing—review & editing, S.I.Y. All authors have read and agreed to the published version of the manuscript.

Funding: This research received no external funding.

Data Availability Statement: All the material conducted in the study is mentioned in article.

Conflicts of Interest: The authors declare no conflict of interest.

References

- Yang, T.; Chi, P.L.; Itoh, T. High isolation and compact diplexer using the hybrid resonators. *IEEE Microw. Wirel. Compon. Lett.* **2010**, *20*, 551–553. [\[CrossRef\]](#)
- Liu, H.; Xu, W.; Zhang, Z.; Guan, X. Compact diplexer using slot line stepped impedance resonator. *IEEE Microw. Wirel. Compon. Lett.* **2013**, *23*, 75–77. [\[CrossRef\]](#)
- Pozar, D.M. *Microwave Engineering*; John Wiley & Sons: Hoboken, NJ, USA, 1998.
- Weng, M.H.; Hung, C.Y.; Su, Y.K. A hairpin line diplexer for direct sequence ultra-wide band wireless communications. *IEEE Microw. Wirel. Compon. Lett.* **2007**, *17*, 519–521. [\[CrossRef\]](#)
- Chen, C.F.; Huang, T.Y.; Chou, C.P.; Wu, R.B. Microstrip diplexers design with common resonator sections for compact size, but high isolation. *IEEE Trans. Microw. Theory Tech.* **2006**, *54*, 1945–1952. [\[CrossRef\]](#)
- Makimoto, M.; Yamashita, S. Bandpass filters using parallel coupled stripline stepped impedance resonators. *IEEE Trans. Microw. Theory Tech.* **1980**, *28*, 1413–1417. [\[CrossRef\]](#)
- Ye, C.S.; Su, Y.K.; Weng, M.H.; Hung, C.Y. A microstripring-like diplexer for bluetooth and UWB application. *Microw. Opt. Tech. Lett.* **2009**, *51*, 1518–1520. [\[CrossRef\]](#)

8. Alanazi, A.K.; Alizadeh, S.M.; Nurgalieva, K.S.; Nestic, S.; Grimaldo Guerrero, J.W.; Abo-Dief, H.M.; Eftekhari-Zadeh, E.; Nazemi, E.; Narozhnyy, I.M. Application of neural network and time-domain feature extraction techniques for determining volumetric percentages and the type of two phase flow regimes independent of scale layer thickness. *Appl. Sci.* **2022**, *12*, 1336. [\[CrossRef\]](#)
9. Nazemi, E.; Roshani, G.; Feghhi, S.; Setayeshi, S.; Zadeh, E.E.; Fatehi, A. Optimization of a method for identifying the flow regime and measuring void fraction in a broad beam gamma-ray attenuation technique. *Int. J. Hydrogen Energy* **2016**, *41*, 7438–7444. [\[CrossRef\]](#)
10. Roshani, G.; Nazemi, E.; Roshani, M. Intelligent recognition of gas-oil-water three-phase flow regime and determination of volume fraction using radial basis function. *Flow Meas. Instrum.* **2017**, *54*, 39–45. [\[CrossRef\]](#)
11. Hosseini, S.; Taylan, O.; Abusurrah, M.; Akilan, T.; Nazemi, E.; Eftekhari-Zadeh, E.; Bano, F.; Roshani, G.H. Application of Wavelet Feature Extraction and Artificial Neural Networks for Improving the Performance of Gas–Liquid Two-Phase Flow Meters Used in Oil and Petrochemical Industries. *Polymers* **2021**, *13*, 3647. [\[CrossRef\]](#) [\[PubMed\]](#)
12. Nazemi, E.; Feghhi, S.; Roshani, G.; Peyvandi, R.G.; Setayeshi, S. Precise void fraction measurement in two-phase flows independent of the flow regime using gamma-ray attenuation. *Nucl. Eng. Technol.* **2016**, *48*, 64–71. [\[CrossRef\]](#)
13. Roshani, G.H.; Roshani, S.; Nazemi, E.; Roshani, S. Online measuring density of oil products in annular regime of gas-liquid two phase flows. *Measurement* **2018**, *129*, 296–301. [\[CrossRef\]](#)
14. Roshani, G.; Hanus, R.; Khazaei, A.; Zych, M.; Nazemi, E.; Mosorov, V. Density and velocity determination for single-phase flow based on radiotracer technique and neural networks. *Flow Meas. Instrum.* **2018**, *61*, 9–14. [\[CrossRef\]](#)
15. Kushwah, V.S.; Tomar, A.S. ANN modeling of microstrip hairpin-line bandpass filter. *Int. J. Commun. Syst. Netw. Technol.* **2014**, *3*, 58–64.
16. Roshani, S.; Azizian, J.; Roshani, S.; Jamshidi, M.B.; Parandin, F. Design of a miniaturized branch line microstrip coupler with a simple structure using artificial neural network. *Frequenz* **2022**, *76*, 255–263. [\[CrossRef\]](#)
17. Parandin, F.; Olyaei, S.; Kamarian, R.; Jomour, M. Design and Simulation of Linear All-Optical Comparator Based on Square-Lattice Photonic Crystals. *Photonics* **2022**, *9*, 459. [\[CrossRef\]](#)
18. Parandin, F.; Sheykhan, A. Design and simulation of a 2×1 All-Optical multiplexer based on photonic crystals. *Opt. Laser Technol.* **2022**, *151*, 108021. [\[CrossRef\]](#)
19. Parandin, F.; Sheykhan, A.; Bagheri, N. A Novel Design for an Ultracompact Optical Majority Gate Based on Ring Resonator on Photonic Crystals Substrate. *J. Comput. Electron.* **2023**, 1–7. [\[CrossRef\]](#)
20. Askarian, A.; Parandin, F. A novel proposal for all optical 1-bit comparator based on 2D linear photonic crystal. *J. Comput. Electron.* **2022**, *22*, 288–295. [\[CrossRef\]](#)
21. Parandin, F.; Heidari, F.; Aslinezhad, M.; Parandin, M.M.; Roshani, S.; Roshani, S. Design of 2D photonic crystal biosensor to detect blood components. *Opt. Quantum Electron.* **2022**, *54*, 618. [\[CrossRef\]](#)
22. Parandin, F.; Mahtabi, N. Design of an ultra-compact and high-contrast ratio all-optical NOR gate. *Opt. Quantum Electron.* **2021**, *53*, 666. [\[CrossRef\]](#)
23. Roshani, S.; Yahya, S.I.; Mezaal, Y.S.; Chaudhary, M.A.; Al-Hilali, A.A.; Ghadi, Y.Y.; Karimi, M.; Roshani, S. Filtering Power Divider A Compact Filtering Coupler with Unwanted Harmonic Rejection Using LC Composite Lines for Communication Systems Applications. *Systems* **2023**, *11*, 14. [\[CrossRef\]](#)
24. Roshani, S.; Yahya, S.I.; Alameri, B.M.; Mezaal, Y.S.; Liu, L.W.; Roshani, S. Filtering Power Divider Design Using Resonant LC Branches for 5G Low-Band Applications. *Sustainability* **2022**, *14*, 12291. [\[CrossRef\]](#)
25. Jamshidi, M.B.; Roshani, S.; Talla, J.; Roshani, S.; Peroutka, Z. Size reduction and performance improvement of a microstrip Wilkinson power divider using a hybrid design technique. *Scientific Reports* **2021**, *11*, 7773. [\[CrossRef\]](#) [\[PubMed\]](#)
26. Karimi, G.; Lalbakhsh, A.; Dehghani, K.; Siahkamari, H. Analysis of novel approach to design of ultra-wide stopband microstrip low-pass filter using modified u-shaped resonator. *ETRI J.* **2015**, *37*, 945–950. [\[CrossRef\]](#)
27. Sariri, H.; Rahmani, Z.; Lalbakhsh, A.; Majidifar, S. Compact LPF using T-shaped resonator. *Frequenz* **2013**, *67*, 17–20. [\[CrossRef\]](#)
28. Wang, Z.; Park, C.W. Multiband pi-shaped structure with resonators for tri-band Wilkinson power divider and tri-band rat-race coupler. In Proceedings of the 2012 IEEE/MTT-S International Microwave Symposium Digest, Montreal, QC, Canada, 17–22 June 2012; pp. 1–3.
29. Dehghani, K.; Karimi, G.; Lalbakhsh, A.; Maki, S.V. Design of lowpass filter using novel stepped impedance resonator. *Electron. Lett.* **2014**, *50*, 37–39. [\[CrossRef\]](#)
30. Zhang, Q.; Zhang, G.; Liu, Z.; Chen, W.; Tang, W. Dual-band filtering power divider based on a single circular patch resonator with improved bandwidths and good isolation. *IEEE Trans. Circuits Syst. II Express Briefs* **2021**, *68*, 3411–3415. [\[CrossRef\]](#)
31. Chen, S.; Qi, S.; Chen, X.; Sun, G.; Wu, W. Five-way radial filtering power divider using back-to-back quarter-mode substrate-integrated waveguide and microstrip resonator. *Electron. Lett.* **2021**, *57*, 888–890. [\[CrossRef\]](#)
32. Moloudian, G.; Lalbakhsh, A.; Bahrami, S. A Harmonic-Free Wilkinson Power Divider Using Lowpass Resonators. In Proceedings of the 2022 16th IEEE European Conference on Antennas and Propagation (EuCAP), Madrid, Spain, 27 March 2022–1 April 2022; pp. 1–4.
33. Lalbakhsh, A.; Afzal, M.U.; Esselle, K.P.; Smith, S.L. Low-cost nonuniform metallic lattice for rectifying aperture near-field of electromagnetic bandgap resonator antennas. *IEEE Trans. Antennas Propag.* **2020**, *68*, 3328–3335. [\[CrossRef\]](#)
34. Azadi, R.; Roshani, S.; Nosratpour, A.; Lalbakhsh, A.; Mozaffari, M.H. Half-elliptical resonator lowpass filter with a wide stopband for low band 5G communication systems. *Electronics* **2021**, *10*, 2916. [\[CrossRef\]](#)

35. Lalbakhsh, A.; Afzal, M.U.; Esselle, K.P.; Smith, S.L. A high-gain wideband EBG resonator antenna for 60 GHz unlicensed frequency band. In Proceedings of the 12th IET European Conference on Antennas and Propagation (EuCAP 2018), London, UK, 9–13 April 2018; pp. 1–3.
36. Lalbakhsh, A.; Afzal, M.U.; Esselle, K.P.; Smith, S.L. An Array of Electromagnetic Bandgap Resonator Antennas for V-Band Backhaul Applications. In Proceedings of the IIER International Conference (248th: 2019), Tokyo, Japan, 7–8 August 2019; The International Institute of Engineers and Researchers: Tokyo, Japan, 2019; pp. 69–71.
37. Wu, H.W.; Huang, S.H.; Chen, Y.F. Design of new quad-channel diplexer with compact circuit size. *IEEE Microw. Wirel. Compon. Lett.* **2013**, *23*, 240–242. [[CrossRef](#)]
38. Chen, F.; Hu, H.; Qiu, J.; Guo, M.; Chu, Q. Novel Diplexer with Improved Isolation Using Asymmetric Transmission Zeros Technique. *Chin. J. Electron.* **2016**, *25*, 591–594. [[CrossRef](#)]
39. Yan, J.M.; Zhou, H.Y.; Cao, L.Z. Compact diplexer using microstrip half-and quarter-wavelength resonators. *Electron. Lett.* **2016**, *52*, 1613–1615. [[CrossRef](#)]
40. Li, J.; Huang, Y.; Zhao, X.; Wen, G. Compact microstrip bandpass diplexer based on twist revised split ring resonators. *Int. J. Antennas Propag.* **2015**, *2015*, 698714. [[CrossRef](#)]
41. Chinig, A.; Zbitou, J.; Errkik, A.; Tajmouati, A.; El Abdellaoui, L.; Latrach, M.; Tribak, A. Microstrip Diplexer Using Stepped Impedance Resonators. *Wirel. Pers. Commun.* **2015**, *84*, 2537–2548. [[CrossRef](#)]
42. Peng, H.S.; Chiang, Y.C. Microstrip diplexer constructed with new types of dual-mode ring filters. *IEEE Microw. Wirel. Compon. Lett.* **2015**, *25*, 7–9. [[CrossRef](#)]
43. Noori, L.; Rezaei, A. Design of a microstrip diplexer with a novel structure for WiMAX and wireless applications. *AEU-Int. J. Electron. Commun.* **2017**, *77*, 18–22. [[CrossRef](#)]
44. Salehi, M.R.; Keyvan, S.; Abiri, E.; Noori, L. Compact microstrip diplexer using new design of triangular open loop resonator for 4G wireless communication systems. *AEU-Int. J. Electron. Commun.* **2016**, *70*, 961–969. [[CrossRef](#)]

Disclaimer/Publisher's Note: The statements, opinions and data contained in all publications are solely those of the individual author(s) and contributor(s) and not of MDPI and/or the editor(s). MDPI and/or the editor(s) disclaim responsibility for any injury to people or property resulting from any ideas, methods, instructions or products referred to in the content.